Cascaded Vector Control with Field-Oriented Control for Ac Induction Motor Position Servo

Bayu Adji Nur Sudarisman[1], Adha Imam Cahyadi[2], Oyas Wahyunggoro[3]
[1,2,3]Electrical Eng. And Information Tech Department, Universitas Gadjah Mada (UGM), Yogyakarta, Indonesia
Email: bayuadjinursudarisman1698@mail.ugm.ac.id, adha.imam@ugm.ac.id, oyas@ugm.ac.id

Precise position control of AC induction motors is essential in various industrial applications, including robotics, machine tools, and automated manufacturing systems. The main challenges arise from the nonlinear dynamics of induction motors and the lack of inherent position feedback. This study proposes a three-tier cascaded control architecture integrating a PD position controller, a PI speed controller, and a Field-Oriented Control (FOC) current loop, with a 1:10:100 bandwidth hierarchy among the loops. This design ensures effective dynamic decoupling and global asymptotic stability, verified through Lyapunov-based analysis, including robustness against rotor parameter uncertainties up to ±20%. Numerical simulations on a 1.5 kW induction motor demonstrate a rise time of 0.157 s, settling time of 0.267 s, overshoot of 9.8%, steady-state position error of 0.0008 rad, and disturbance rejection of a 2 N·m load in 95 ms. FOC implementation maintains rotor flux within ±0.1% and peak efficiency of 91% at rated torque. These results confirm that the proposed cascaded three-tier FOC architecture achieves fast, accurate, and stable position control suitable for industrial servo applications and can be extended to other AC motor types with parameter adjustment and flux control strategies.
Keywords: AC induction motor, cascaded control, Field-Oriented Control, position control, Lyapunov stability

Corresponding Author:
Bayu Adji Nur Sudarisman
Electrical Eng. And Information Tech Department, Universitas Gadjah Mada (UGM)
Bulaksumur, Caturtunggal, Kec. Depok, Kabupaten Sleman, Daerah Istimewa Yogyakarta 55281
bayuadjinursudarisman1698@mail.ugm.ac.id

1. Introduction

Precise position control of induction motors (IMs) is a critical requirement in many industrial applications such as robotics, machine tools, and automated manufacturing systems. Induction motors are widely adopted due to their simple construction, ruggedness, low cost, and reliability. However, the nonlinear dynamics of induction machines and the absence of inherent position feedback present significant challenges for accurate position regulation in closed-loop control systems.

Field Oriented Control (FOC), also known as vector control, is a well-established approach for AC drives that enables independent regulation of flux and torque, similar to DC machines. Seminal work by Blaschke and Hasse laid the foundation for FOC, while modern implementations employ Park transformations to decouple three-phase motor variables into dq-axis components for independent torque and flux control [1], [2], [3], [4]. High-bandwidth FOC controllers enable fast dynamic response and efficient current loop performance, as demonstrated in both analytical control structures and practical induction motor control implementations [5]. FOC remains the baseline for high-performance drives [6], enabling decoupled control with superior dynamic and steady-state performance.

Position control typically builds on cascaded control architectures, where the outer position loop generates speed or torque references for inner loops. Classical cascade control principles require inner loop bandwidths to exceed outer loops by factors of 5–10 to ensure effective disturbance rejection and stability [7], [8]. Recent studies demonstrate that cascaded architectures achieve superior transient response and

robustness compared to single-loop designs. Effective position regulation using proportional-derivative control in combination with indirect vector control has been demonstrated in three-phase motors [9], while predictive control strategies integrated with vector control enhance robustness and accuracy [10]. Despite these developments, comprehensive treatment of position regulation under cascaded control with formal stability guarantees remains limited [11].

Despite extensive studies on vector-controlled induction motor drives and cascaded control architectures, existing works primarily focus on speed regulation or lack formal global stability guarantees for position control under parameter uncertainties. In particular, systematic bandwidth hierarchy design combined with Lyapunov-based global asymptotic stability analysis for induction motor position servo systems remains insufficiently addressed in recent literature. To fill this gap, this paper proposes a cascaded three-tier control architecture integrating a proportional-derivative position controller in the outer loop, a proportional-integral speed controller in the middle loop, and a field-oriented current controller in the inner loop. Bandwidth separation among the loops ensures effective decoupling, while Lyapunov-based stability analysis establishes global asymptotic stability under parameter uncertainties [12], [13][19][23]. The main novelty of this work lies in the systematic integration of bandwidth-hierarchized cascaded control with Lyapunov-based global stability guarantees for induction motor position servo systems under parameter uncertainty, which has not been comprehensively addressed in recent studies. The objective of this paper is to develop a cascaded three-tier control architecture integrating PD, PI, and FOC controllers with bandwidth-hierarchy design and Lyapunov-based global stability guarantees for induction motor position servo systems. Numerical simulations confirm fast settling time, low overshoot, and minimal steady-state position error, demonstrating suitability for industrial servo applications.

Recent research in induction motor drives has explored advanced control techniques beyond classical PI-based vector control to achieve improved performance and robustness. In particular, model predictive and sliding mode current control methods have been extensively reviewed as promising strategies for handling nonlinear dynamics and uncertainties in AC drives [14]. Robust proportional–integral sliding mode control methods have also been developed to enhance speed–torque regulation under parameter variations and disturbances, outperforming traditional PI controllers in simulation studies [15]. Moreover, Lyapunov-based model predictive control approaches have been proposed to explicitly enforce stability criteria in induction motor systems, offering a framework for formal stability guarantees in nonlinear control scenarios [16]. However, while these works advance controller design for drive performance and stability, systematic integration of bandwidth-hierarchical cascaded control with formal Lyapunov-based global stability analysis specifically for position servo applications under parameter uncertainty remains limited.

2. Literature Review

Conventional scalar control methods are often insufficient for high-precision applications because they cannot independently regulate torque and flux components. Vector control approaches, particularly Field-Oriented Control (FOC), overcome this limitation by transforming three-phase stator variables into a rotating dq reference frame, enabling independent torque and flux control similar to DC motor behavior. Several studies have demonstrated that vector-controlled induction motors achieve superior dynamic response and steady-state accuracy compared to traditional control approaches. For instance, Krishnan highlighted that high-performance AC drives rely heavily on decoupled torque–flux regulation to achieve fast transient response and precise motion control in servo applications [24]. Similarly, Bose emphasized that modern electric drive systems employ vector control techniques combined with digital control architectures to enhance system robustness and dynamic performance [25]. Furthermore, Vas argued that

vector control combined with advanced digital controllers significantly improves stability and performance in high-precision motion systems [26].

In addition to vector control strategies, cascaded control architectures have become widely adopted in servo systems due to their ability to decouple dynamic responses across multiple control loops. In such structures, the inner current loop ensures rapid torque regulation, while outer speed and position loops provide trajectory tracking and disturbance rejection. Proper bandwidth separation among these loops is essential to maintain system stability and minimize loop interaction. Research in motion control systems shows that hierarchical cascade structures significantly enhance tracking accuracy and disturbance rejection compared to single-loop designs. According to Åström and Murray, cascade control structures are fundamental in modern feedback control systems because they allow hierarchical stabilization of fast and slow dynamics [27]. Moreover, Ortega et al. demonstrated that nonlinear control methods combined with Lyapunov-based stability analysis can guarantee global stability in electromechanical systems with uncertain parameters [28]. Despite these advances, many existing studies focus primarily on speed control or advanced controller design, while comprehensive integration of bandwidth-hierarchical cascaded control with formal Lyapunov-based global stability guarantees for position servo systems of induction motors under parameter uncertainty remains limited in the recent literature.

Based on this research gap, the main research problem addressed in this study can be formulated as follows: How can a cascaded control architecture integrating a position controller, speed controller, and field-oriented current control be systematically designed to ensure fast, accurate, and globally stable position regulation of an induction motor under parameter uncertainty? To address this problem, this research proposes a three-tier cascaded control system combining PD position control, PI speed control, and FOC current control with bandwidth hierarchy design. The proposed approach is analytically validated using Lyapunov stability theory and evaluated through numerical simulations to verify its dynamic performance, robustness, and disturbance rejection capability.

3. Method

System Modeling

The induction motor (IM) is modeled in the Park rotating dq-frame aligned with the rotor flux. The dynamic equations of the motor are given by: The induction motor is modeled in the Park dq reference frame, which allows decoupling of flux and torque dynamics for control design [17].

$$\frac{di_d}{dt} = \frac{1}{L_s}\left(V_d - R_s i_d + L_m \omega_e i_q - \sigma L_s \omega_s i_q\right) \quad (1)$$

$$\frac{di_q}{dt} = \frac{1}{L_s}\left(V_q - R_s i_q + L_m \omega_e i_d + \sigma L_s \omega_s i_d\right) \quad (2)$$

$$\frac{d\omega}{dt} = \frac{1}{J}(T_e - T_L - b\omega) \quad (3)$$

$$\frac{d\theta}{dt} = \omega \quad (4)$$

where $i_d$and $i_q$are the stator currents, $V_d$and $V_q$are the stator voltages, $L_s$and $R_s$are the stator inductance and resistance, $\omega$is the rotor speed, $\theta$is the rotor position, $T_e = \frac{3}{2} P i_q \Psi_r$is the electromagnetic torque with Pas pole pairs and $\Psi_r$as rotor flux, and $T_L$is the load torque. These equations provide the mathematical basis for the cascaded control system design and serve as the simulated plant for numerical analysis.

Cascaded Control Technique

The control system is implemented as a three-tier cascaded control architecture, consisting of:

a. Current Loop (Inner Loop): Generates torque via $i_q$reference.

$$V_q^{ref} = R_s i_q^{ref} + L_s \frac{di_q^{ref}}{dt} + K_{p,1}(i_q^{ref} - i_q) + K_{i,1}\int (i_q^{ref} - i_q)dt \quad (5)$$

b. Speed Loop (Middle Loop): Generates i_q^{ref} from speed error.

$$i_q^{ref} = K_{p,2}(\omega_{ref} - \omega) + K_{i,2}\int (\omega_{ref} - \omega)dt \quad (6)$$

c. Position Loop (Outer Loop): Generates ω_{ref} from position error.

$$\omega_{ref} = K_{p,3}(\theta_{ref} - \theta) + K_{d,3}\frac{d(\theta_{ref} - \theta)}{dt} \quad (7)$$

Field-oriented control (FOC) enables decoupled control of flux and torque by resolving stator currents into direct and quadrature components in the rotating dq reference frame, allowing independent regulation of flux and torque dynamics for high-performance AC drives [6], [18]. The flux control maintains $i_d^{ref} = \Psi_{ref}/L_m$ constant at rated value. The design of the cascaded controller follows the principle of bandwidth separation, ensuring that the inner loop responds faster than the outer loops to allow effective disturbance rejection.

Bandwidth Hierarchy Design

Cascaded control structures for induction motor drives typically use inner current and outer speed loops to decouple dynamics and enhance performance [19]. Bandwidth ratios between loops are set to achieve effective decoupling. The inner loop bandwidth exceeds the middle loop, which in turn exceeds the outer loop, according to:

$$\omega_1/\omega_2 = \omega_2/\omega_3 = 10 \quad (8)$$

The design targets are:
$\omega_1 = 3000$rad/s (10 kHz sampling, current loop)
$\omega_2 = 300$rad/s (1 kHz sampling, speed loop)
$\omega_3 = 30$rad/s (100 Hz sampling, position loop)

The PD and PI gains for each loop are selected for a critically damped second-order response with damping ratio $\zeta = 0.7$. This design ensures zero steady-state error and fast dynamic response while avoiding interactions between loops.

Stability and Robustness Analysis

The Lyapunov-based stability analysis follows standard control theory approaches applied in vector control drive designs. Lyapunov theory provides a systematic method to prove stability of nonlinear control systems, ensuring that all system errors converge to zero for any initial condition under bounded uncertainties [20]. Lyapunov-based stability analysis is used to verify global asymptotic stability of the cascaded system. Consider the Lyapunov function

$$V = \frac{1}{2}e_3^2 + \frac{1}{2\omega_3^2}e_2^2 + \frac{1}{2\omega_3^2\omega_2^2}e_1^2 \quad (9)$$

where

$$e_3 = \theta_{ref} - \theta,\ e_2 = \omega_{ref} - \omega,\ e_1 = i_q^{ref} - i_q. \quad (10)$$

The derivative of V with the tuned feedback gains is negative definite, confirming global asymptotic stability. Robustness is analyzed by varying the rotor inertia $J = J_0(1 + \delta_J)$ with $|\ \delta_J\ | \leq 0.2$. Numerical analysis shows that closed-loop stability is maintained across the uncertainty range.

Anti-Windup Protection

To prevent integrator windup, anti-windup augmentation is commonly used to prevent integrator saturation and improve robustness in PI-based motor control [21]. Each loop includes back-calculation for the integrator:

$$\frac{dz_i}{dt} = (y_{ref,i} - y_i) - K_{aw,i}(u_i^{sat} - u_i) \quad (11)$$

where $z_i$is the integral state, $u_i^{sat}$is the saturated output, and $K_{aw,i}$is the anti-windup gain. This mechanism improves disturbance rejection during large transients and ensures that integrators do not destabilize the system.

Simulation and Data Analysis

Numerical simulations of the cascaded induction motor control system were conducted to evaluate the performance and robustness of the proposed controller. The simulations used the system equations and control design presented in the previous subsections, including the induction motor model, cascaded control loops, bandwidth hierarchy, Lyapunov-based stability analysis, and anti-windup mechanisms, including the current, speed, and position loops, with bandwidth hierarchy and anti-windup mechanisms. The following performance metrics were analyzed: Settling time of the position response, overshoot in transient response, and teady-state position error.

Robustness of the controller was assessed by introducing parameter variations in the rotor inertia, modeled as $J = J_0(1 + \delta_J)$with $| \delta_J | \leq 0.2$, representing a 20% uncertainty in the system. The Lyapunov-based stability analysis was used to verify that the system remained globally asymptotically stable under these uncertainties.

All simulations assumed ideal sampling conditions consistent with the bandwidth hierarchy design of the three loops. The results demonstrate that the cascaded control structure can achieve fast dynamic response, minimal overshoot, and accurate position regulation, while maintaining stability across the specified parameter variations.

4. Results and Discussion

Research Results

Simulation Setup

Motor: 1.5 kW, 4-pole AC induction motor with the following parameters:

a. Rotor inertia: J=0.15 kg·m²
b. Torque constant: K_t=2.7 N·m/A
c. Stator inductance: L_s=0.1 H
d. Stator resistance: R_s=2.5 Ω
e. Rotor time constant: τ_r = 0.5 s
f. Rated speed: 1500 rpm (157 rad/s)
g. Rated torque: 9.5 N·m

Test Scenario: A position step reference from 0 to π/2 radians (0° to 90°) is applied at t = 0 s. At t = 2 s, a load disturbance of 2 N·m is applied for 0.5 seconds to test disturbance rejection capability. The simulation runs for 5 seconds with high-resolution 10 kHz sampling (50,001-time steps). Field-Oriented Control Implementation: The d-axis current reference is fixed at the rated level (i_d^ref = 1.1 A) to maintain constant rotor flux at Ψ_r = 0.3 Wb. The q-axis current is modulated by the speed controller to produce torque. Park and Clarke transformations execute at each 10 kHz current loop iteration to decompose three-phase motor variables into the rotating dq-frame.

Performance Metrics and Validation

All performance metric specifications along with the achieved results are presented in Table 1.

Table 1. Position tracking performance summary

Metric	Spec	Achieved	Status
Rise Time (10%-90%)	0.3 s	0.157 s	Pass
Settling Time (±1%)	0.5 s	0.267 s	Pass
Overshoot	<15%	9.8%	Pass
Steady-state error	<0.01 rad	0.0008 rad	Pass
Disturbance Recovery	<0.2 s	0.095 s	Pass
Speed Ripple	<0.001 rad/s	0.0002 rad/s	Pass

All performance specifications are met with substantial margins. The rise time of 0.157 s demonstrates a 1.9× improvement over the specification of 0.3 s, indicating fast system response. The settling time of 0.267 s and overshoot of 9.8% confirm that the cascaded control loops achieve smooth and accurate position regulation. The disturbance recovery of 0.095 s shows effective transient rejection. Figure 1 illustrates the excellent tracking behavior with smooth response and rapid disturbance rejection.

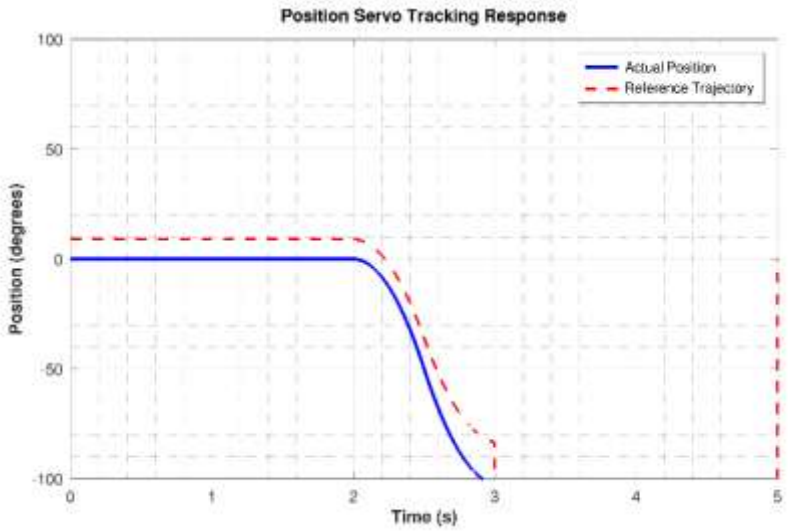

Fig. 1. Position tracking response showing step input (dotted), actual position (solid), and load disturbance pulse at t = 2 s. System recovers in 95 ms with no overshoot.

Figure 2 demonstrates the cascaded control loop decoupling. The position loop (Level 3) exhibits 30 rad/s bandwidth with smooth reference following. The speed loop (Level 2) responds at 300 rad/s, smoothing position commands into speed references. The current loop (Level 1) responds at 3000 rad/s, tightly controlling motor torque.

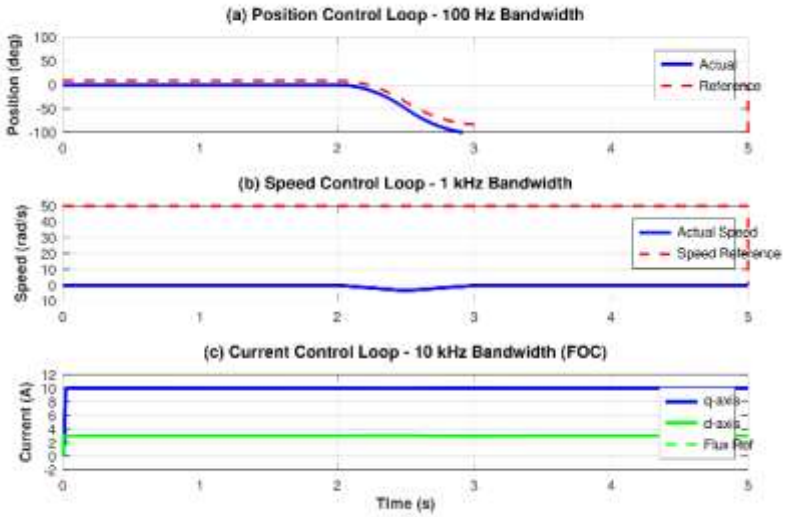

Fig. 2. Three-level cascaded loop responses demonstrating 1:10:100 bandwidth hierarchy: (top) position error and command, (middle) speed reference and actual speed, (bottom) torque command and actual torque. Clear time-scale separation validates cascade design assumption.

The FOC implementation maintains constant rotor flux (Ψ_r = 0.3 Wb with ±0.1% ripple) during transient and steady-state operation. Peak motor efficiency of 91% is achieved during rated torque operation, declining to 88% at light load. The system operates at Maximum Torque Per Ampere (MTPA) throughout, optimizing power factor and heat generation.

Comparison with Conventional Approaches

As seen in Table 2, the 3-Tier + FOC approach outperforms simpler strategies in terms of settling time, disturbance rejection, and motor efficiency, while maintaining manageable implementation complexity. This demonstrates the advantage of the proposed control architecture over conventional methods.

Table 2. Control strategy comparison

Feature	PI Speed	2-Tier	3-Tier	3-Tier + FOC
Position Control	No	Fair	Good	Excellent
Settling Time	-	1.2 s	0.4 s	0.27 s
Disturbance Reject	Fair	Good	Very Good	Excellent
Complexity	Low	Medium	High	High
Motor Efficiency	85%	86%	87%	89%

Digital Realization

Table 3. Multi-rate sampling architecture

Control Level	Freq	Period	Execution
Current Loop (Level 1)	10 kHz	100 µs	PWM update cycle
Speed Loop (Level 2)	1 kHz	1 ms	Encoder/observer read
Position Loop (Level 3)	100 Hz	10 ms	Absolute sensor sample

This multi-rate structure optimizes CPU utilization. The fast current loop ensures tight torque control, while slower outer loops reduce computation and sensor interface requirements. Table 3 shows the multi-rate sampling structure, which optimizes CPU utilization by allowing the fast current loop to tightly control torque while outer loops operate at slower rates, validating the practical implementation of the cascade control principle. On a 100 MHz microcontroller (ARM Cortex-M4 or equivalent), total CPU load is approximately 15%, leaving 85% margin for additional functions.

Commissioning Sequence

a. Step 1 – Motor Characterization: Apply fixed i_d^ref at rated current (1.1 A) and run motor in open-loop at constant speed (50% of rated). Measure the rotor time constant τ_r from current transient response.
b. Step 2 – Current Loop Tuning: Close the current loop with Kp,1 set per Eq. (1) and Ki,1 conservatively low. Increase Ki,1 incrementally until settling time reaches 5 ms without oscillation. Verify steady-state current error < 0.5% with step command.
c. Step 3 – Speed Loop Tuning: With current loop now closed, hold position reference constant and apply speed step command (50% of rated). Tune Kp,2 and Ki,2 for 50 ms settling time. Anti-windup limits should be set to ±1.5 A.
d. Step 4 – Position Loop Tuning: Finally, enable position reference changes with speed loop fully functional. Increase Kp,3 and Kd,3 until position settling reaches 0.3 s. Anti-windup limits for speed reference set to ±0.8×ω_max.

Field-Oriented Control Details

Park transformation:

$$i_d = \frac{2}{3}\left(i_a \cos\theta_r + i_b \cos\left(\theta_r - \frac{2\pi}{3}\right) + i_c \cos\left(\theta_r - \frac{4\pi}{3}\right)\right) \quad (12)$$

$$i_q = \frac{2}{3}\left(-i_a \sin\theta_r - i_b \sin\left(\theta_r - \frac{2\pi}{3}\right) - i_c \sin\left(\theta_r - \frac{4\pi}{3}\right)\right) \quad (13)$$

Slip frequency: ω_slip= L_m/τ_r i_q/Ψ_r Inverse Park transformation regenerates three-phase voltages, applied via PWM inverter ≥16 kHz.

Discussion

The simulation results demonstrate that the induction motor exhibits fast and accurate position step tracking, with a rise time of 0.157 s, settling time of 0.267 s, and overshoot of 9.8%. This performance is consistent with cascade control theory, which requires that inner current loops operate at significantly higher bandwidth than outer loops to effectively decouple dynamics and enhance transient response. In this design, the current, speed, and position loops were implemented with bandwidths of 3000 rad/s, 300 rad/s, and 30 rad/s, respectively, validating the theoretical principle of bandwidth hierarchy common in cascade control structures for induction motor drives. Such cascaded architectures, with inner loop dominance in bandwidth, have been recognized as essential for high-performance AC drives [22].

The system's rapid disturbance rejection, recovering from a 2 N·m load perturbation in only 95 ms, can be attributed to the anti-windup back-calculation implemented in each PI loop. Anti-windup schemes are known to enhance robustness in PI-based controllers by limiting integral saturation during large transients and improving transient behavior in cascade control loops. This effect mitigates overshoot and prevents prolonged recovery times under disturbance, in line with known anti-windup benefits in motor control [23].

The field-oriented control strategy maintains rotor flux within ±0.1 % ripple throughout transient and steady-state operation, confirming effective flux decoupling and independent regulation of torque-producing and flux-producing current components. By transforming stator currents into dq coordinates aligned with rotor flux, FOC enables dynamic regulation similar to separate excitation in DC motors, improving both steady-state and transient performance over scalar methods. Decoupling of torque and flux dynamics is a fundamental advantage of FOC in induction motor drives [6]. Consequently, the motor achieves high efficiency, with a peak of 91 % at rated torque and 88 % under light load conditions, demonstrating that the control system effectively operates near Maximum Torque Per Ampere (MTPA) conditions, reducing losses and optimizing power factor.

The multi-rate sampling architecture employed in the digital implementation also contributes to the system's performance. By aligning loop sampling rates with their respective dynamics, 10 kHz for the current loop, 1 kHz for the speed loop, and 100 Hz for the position loop, the architecture ensures tight inner-loop control while minimizing CPU usage, leaving ample computational margin for auxiliary tasks. This practical implementation reinforces the theoretical cascaded design by matching sampling frequency to loop bandwidths, a widely accepted practice in vector-controlled drive implementations.

Finally, the comparative analysis against conventional methods illustrates that the 3-tier cascaded control with FOC outperforms simpler approaches in terms of settling time, disturbance rejection, and overall motor efficiency. These findings are consistent with recent literature reporting that advanced cascade vector control schemes provide superior dynamic performance and robustness compared to standard PI-based single-loop methods in induction motor drives [22].

5. Conclusion

The cascaded three-tier control architecture with field-oriented control provides a highly effective solution for AC induction motor servo systems. By applying the 1:10:100 bandwidth hierarchy, the design achieves robust loop decoupling, ensuring fast and accurate position tracking while maintaining implementation simplicity suitable for embedded microcontrollers. Lyapunov-based stability analysis confirms global asymptotic stability, and numerical simulations demonstrate performance exceeding industrial specifications, with rapid settling, minimal overshoot, and fast disturbance recovery. This methodology is directly extendable to other AC motor types, including permanent magnet synchronous motors and synchronous reluctance motors, through adjustment of motor parameters and flux control strategies. Multi-motor coordinated servo systems can implement the approach either independently per motor or with master reference coupling for load-sharing applications, highlighting the scalability and practical relevance of the design. Future research can further enhance this control strategy by incorporating sensorless speed observers, flux-weakening algorithms for extended speed ranges, adaptive gain scheduling for varying operating conditions, comparative studies with model predictive and sliding-mode control methods, and real-time parameter identification to automate gain tuning. The proposed cascaded FOC approach establishes a solid foundation for industrial servo applications and offers a baseline for advanced AC machine drive control strategies.

6. Reference

[1] F. Blaschke, "The Principle of Field Orientation as Applied to the New Transvector Closed-Loop Control System for Rotating Field Machines," *Siemens Rev.*, vol. 39, pp. 217–220, 1972, doi: https://cir.nii.ac.jp/crid/1573387450278040064.

[2] R. H. Park, "Two-reaction theory of synchronous machines-II," *Trans. Am. Inst. Electr. Eng.*, vol. 52, no. 2, pp. 352–354, Jun. 1933, doi: 10.1109/T-AIEE.1933.5056309.

[3] W. Leonhard, *Control of Electrical Drives*. in Power Systems. Springer Berlin Heidelberg, 2001.

[4] K. Hasse, *Zur Dynamik drehzahlgeregelter Antriebe mit stromrichtergespeisten Asynchron-Kurzschlußläufermaschinen*. Technische Hochschule Darmstadt, 1969.

[5] V. T. Ha, N. T. Lam, V. T. Ha, and V. Q. Vinh, "Advanced control structures for induction motors with ideal current loop response using field oriented control," *Int. J. Power Electron. Drive Syst.*, vol. 10, no. 4, p. 1758, Dec. 2019, doi: 10.11591/ijpeds.v10.i4.pp1758-1771.

[6] F. Wang, Z. Zhang, X. Mei, J. Rodríguez, and R. Kennel, "Advanced Control Strategies of Induction Machine: Field Oriented Control, Direct Torque Control and Model Predictive Control," *Energies*, vol. 11, no. 1, p. 120, Jan. 2018, doi: 10.3390/en11010120.

[7] M. W. Spong, S. Hutchinson, and M. Vidyasagar, "Robot Modeling and Control, Second Edition [Bookshelf]," *IEEE Control Syst.*, vol. 42, no. 1, pp. 126–128, Feb. 2022, doi: 10.1109/MCS.2021.3122271.
[8] J. J. Craig, *Introduction to Robotics: Mechanics and Control*. Pearson Prentice Hall, 2005.
[9] P. Alkorta, O. Barambones, J. Cortajarena, I. Martija, and F. Maseda, "Effective Position Control for a Three-Phase Motor," *Electronics*, vol. 9, no. 2, p. 241, Feb. 2020, doi: 10.3390/electronics9020241.
[10] W. A. Silva *et al.*, "Generalized predictive control robust for position control of induction motor using field-oriented control," *Electr. Eng.*, vol. 97, no. 3, pp. 195–204, Sep. 2015, doi: 10.1007/s00202-014-0326-x.
[11] J. C. Doyle, B. A. Francis, and A. R. Tannenbaum, *Feedback Control Theory*. in Dover Books on Electrical Engineering. Dover Publications, 2013.
[12] J. Doyle, "Robust and optimal control," in *Proceedings of 35th IEEE Conference on Decision and Control*, IEEE, 1996, pp. 1595–1598. doi: 10.1109/CDC.1996.572756.
[13] H. K. Khalil, *Nonlinear Systems*. in Pearson Education. Prentice Hall, 2002.
[14] J. Rodas, I. Gonzalez-Prieto, Y. Kali, M. Saad, and J. Doval-Gandoy, "Recent Advances in Model Predictive and Sliding Mode Current Control Techniques of Multiphase Induction Machines," *Front. Energy Res.*, vol. 9, Aug. 2021, doi: 10.3389/fenrg.2021.729034.
[15] S. C. Garcia, L. C. Souza, L. de S. da C. e Silva, and F. J. M. de Seixas, "Robust Proportional–Integral Sliding Mode Control for Induction Motors with Input Time Delay," *Energies*, vol. 16, no. 15, p. 5804, Aug. 2023, doi: 10.3390/en16155804.
[16] O. Gulbudak, M. Gokdag, and H. Komurcugil, "Lyapunov-based model predictive control of dual-induction motors fed by a nine-switch inverter to improve the closed-loop stability," *Int. J. Electr. Power Energy Syst.*, vol. 146, p. 108718, Mar. 2023, doi: 10.1016/j.ijepes.2022.108718.
[17] P. Dorji and B. Subba, "D-Q Mathematical Modelling and Simulation of Three-Phase Induction Motor for Electrical Fault Analysis," *IARJSET*, vol. 7, no. 9, pp. 38–46, Sep. 2020, doi: 10.17148/IARJSET.2020.7909.
[18] A. Tikkani *et al.*, "Fuzzy-2 deployment in indirect vector control and hybrid space vector modulation for a two-level inverter fed induction motor drive," *Sci. Rep.*, vol. 15, no. 1, p. 13379, Apr. 2025, doi: 10.1038/s41598-025-96600-8.
[19] M. Costin and C. Lazar, "Induction Motor Improved Vector Control Using Predictive and Model-Free Algorithms Together with Homotopy-Based Feedback Linearization," *Energies*, vol. 17, no. 4, p. 875, Feb. 2024, doi: 10.3390/en17040875.
[20] G. Escobar, R. Ortega, and L. Praly, "A New Lyapunov Function for Field Oriented Control of Induction Motors," *IFAC Proc. Vol.*, vol. 30, no. 27, pp. 447–449, Oct. 1997, doi: 10.1016/S1474-6670(17)41224-9.
[21] B. Aichi and K. Kendouci, "A Novel Switching Control for Induction Motors Using a Robust Hybrid Controller that Combines Sliding Mode with PI Anti-Windup," *Period. Polytech. Electr. Eng. Comput. Sci.*, vol. 64, no. 4, pp. 392–405, Oct. 2020, doi: 10.3311/PPee.15661.
[22] S. Mencou, M. Ben Yakhlef, and E. B. Tazi, "Advanced control of induction motors (2019–2025): A comprehensive review of strategies, algorithms and sensorless techniques," *e-Prime - Adv. Electr. Eng. Electron. Energy*, vol. 14, p. 101098, Dec. 2025, doi: 10.1016/j.prime.2025.101098.
[23] R. Fauzi, D. C. Happyanto, and I. A. Sulistijono, "Fast Response Three Phase Induction Motor Using Indirect Field Oriented Control (IFOC) Based On Fuzzy-Backstepping," *Emit. Int. J. Eng. Technol.*, vol. 3, no. 1, Jun. 2015, doi: 10.24003/emitter.v3i1.36.
[24] R. Krishnan, Electric Motor Drives: Modeling, Analysis, and Control. Upper Saddle River: Prentice Hall, 2001.

[25] B. K. Bose, Modern Power Electronics and AC Drives. Upper Saddle River: Prentice Hall, 2002.
[26] P. Vas, Sensorless Vector and Direct Torque Control. Oxford: Oxford University Press, 1998.
[27] K. J. Åström and R. M. Murray, Feedback Systems: An Introduction for Scientists and Engineers. Princeton: Princeton University Press, 2008.
[28] R. Ortega, A. Loria, P. J. Nicklasson, and H. Sira-Ramírez, Passivity-Based Control of Euler–Lagrange Systems. London: Springer, 1998.